



Characteristics of heat and mass transport in a passive direct methanol fuel cell operated with concentrated methanol

Ya-Ling He*, Zheng Miao, Wei-Wei Yang

Key Laboratory of Thermo-Fluid Science and Engineering of MOE, School of Energy and Power Engineering, Xi'an Jiaotong University, Xi'an, Shaanxi 710049, People's Republic of China

ARTICLE INFO

Article history:

Received 10 December 2011
Received in revised form 8 February 2012
Accepted 11 February 2012
Available online 19 February 2012

Keywords:

Direct methanol fuel cell
High-concentration
Methanol vapor transport layer
Water management layer

ABSTRACT

In this work, the effect of cell structure on the overall cell performance as well as the heat and mass transport in a passive direct methanol fuel cell (DMFC) operated with concentrated methanol solution is experimentally investigated. The influences of the anode methanol vapor transport layer (VTL) and cathode water management layer (WML) are examined. The variations of cell temperature under different working conditions are also recorded. The results show that both the anode VTL thickness and cathode WML thickness greatly influence the cell performance and the species transport in the cell, which should be carefully optimized. Also, it is shown that the difference between the stable cell temperature under the open circuit condition and that under constant voltage discharging condition is quite small for a passive vapor-feed DMFC operated with concentrated fuel. Theoretical analysis and experimental results show that the transport resistance of methanol in the membrane electrode assembly (MEA) is much smaller than that in the other anode components of the cell structure.

© 2012 Elsevier B.V. All rights reserved.

1. Introduction

A direct methanol fuel cell (DMFC) converts chemical energy stored in methanol directly into electricity. It has been regarded as one of the most promising power sources for portable and mobile devices because of its advantages such as high energy density, simple structure, and easy fuel storage and recharging [1,2]. However, the wide application of DMFCs is still hindered by several technical challenges [3–9], including the sluggish kinetics of the anode methanol oxidation reaction, mixed potential on the cathode electrode caused by methanol crossover, and effective water and thermal management. To alleviate the risk of catalyst poisoning and severe methanol crossover problem, diluted methanol solutions (0.5–1 M for the active DMFCs and 2–4 M for the passive DMFCs) [10,11] are usually fed to the DMFC anode such that a fairly good cell performance can be achieved. However, the inherent advantage of high specific energy of the DMFC is significantly sacrificed. Recently, more and more efforts have been made to develop high-concentration DMFC [12–29], i.e. operating DMFC with highly concentrated methanol solution or neat methanol.

To operate a DMFC with highly concentrated fuel, the methanol concentration in the anode catalyst layer (CL) should be controlled at an appropriate level to depress the adverse impact of methanol

crossover and simultaneously meet the requirement of anode reaction. Nakagawa and his co-workers [12–14] designed a fuel delivery system for high-concentration DMFC which consists of a methanol solution reservoir, a hydrophobic porous carbon plate of high mass transport resistance of liquid and gas phases, and a perforated current collector. With the optimization of the pore size in the porous carbon plate, the CO₂ generated in the anode electrochemical reaction can be trapped in the holes of the current collector to form a gas-rich barrier. Thus, methanol in the reservoir should diffuse through this barrier as a vapor-phase to the anode CL. As a result, the methanol concentration in the anode CL can be controlled. With this design, the 22 M methanol solution can be used. Ren et al. [15] proposed a unique DMFC design that can be operated with neat methanol. The key component in this design is the so called “pervaporation film”, which is located between the fuel reservoir and methanol vapor diffusion chamber. This film can vaporize liquid methanol to methanol vapor and limit the delivery rate of methanol from the reservoir to the anode CL. A similar design was proposed by Kim [16] which uses a Nafion membrane as the pervaporation film and adds a barrier and a buffer to further control the methanol delivery rate. They claimed that this design enable the DMFC operating with neat methanol at the power density ranging from 25 to 30 mW cm⁻² for about 360 h. Several similar designs are also reported by other researcher [17,18]. Recently, Wu et al. [19] also proposed a novel micro-fluidic flow field design to allow the passive DMFC running with high-concentration methanol solution. By using this micro-fluidic flow field, the 18 M methanol solution

* Corresponding author. Tel.: +86 29 8266 5930; fax: +86 29 8266 9106.
E-mail address: yalinghe@mail.xjtu.edu.cn (Y.-L. He).

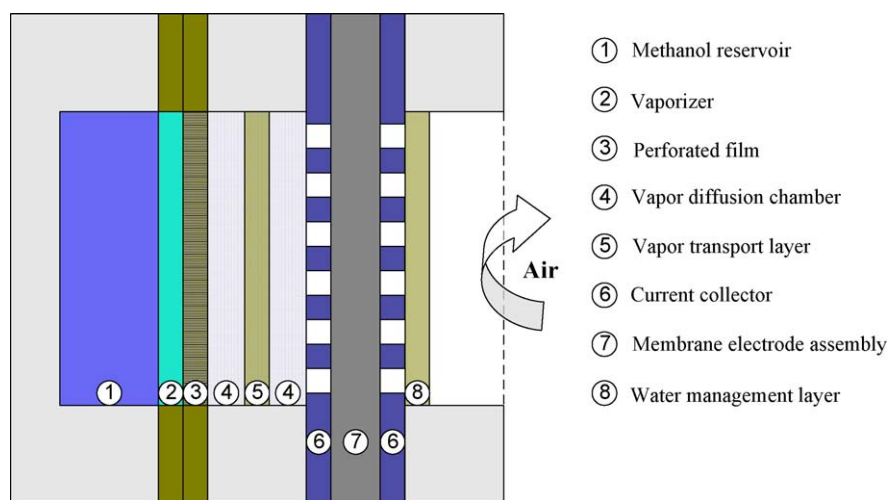


Fig. 1. Schematic of the structure of the passive vapor-feed high-concentration DMFC.

can be fed to the DMFC and a fairly good cell performance can be achieved.

Besides the control of the anode methanol transport, the transport of water also needs to be properly managed. On one hand, the polymer electrolyte membrane should be properly humidified to maintain a relatively high proton conductivity. On the other hand, sufficient water should be kept in the anode CL in order to obtain a high methanol oxidization reaction (MOR) rate. As water supply to the anode is insufficient in the high-concentration DMFC, recovering part of the water produced in the cathode CL to the anode is thus required [10,20–23]. Xu et al. [24] tested the performance of a passive vapor-feed high-concentration DMFC with a membrane vaporizer, a hydrophobic methanol vapor transport layer (VTL) at the anode and a water management layer (WML) at the cathode. The effects of the structure parameters, including the VTL thickness, open ratio of the vaporizer and the WML were investigated. It was indicated that the WML at the cathode is useful in lowering the methanol crossover and increasing the membrane hydration level. Wu et al. [25–27] proposed a method to in situ determine the water transport rate through the membrane in a vapor-feed high-concentration DMFC. Also, effects of the design parameters of the membrane electrode assembly (MEA) and operating conditions on water transport rate as well as the cell performance were studied. In addition, they proposed a unique MEA design to improve the water recovery from the cathode CL to the anode CL, in which a thin layer consisting of nano-sized SiO_2 particles and Nafion ionomer was coated on each side of the membrane. Li et al. [28,29] optimized the cell structure of a liquid-feed high-concentration DMFC by adding a thick porous PTFE plate with high transport resistance. This porous PTFE plate enables the methanol concentration in the anode CL to be controlled at the adequate level.

The above literature review shows that the performance of the DMFC operated with concentrated methanol is sensitively influenced by the design of the cell structure. Although various designs are proposed, the effect of the design parameters on the species transport has not yet been well understood. In addition, the heat transfer behavior in the high-concentration DMFC also needs to be investigated. In this work, we designed a passive vapor-feed high-concentration DMFC with using a pervaporation film. The effects of the VTL thickness and the WML thickness on the species transport as well as the overall cell performance are investigated. Also, the temperature variations of the DMFC under different operation conditions are tested.

2. Experimental

2.1. Cell structure of the DMFC

The schematic of this passive vapor-feed high-concentration DMFC is presented in Fig. 1. The fuel delivery part of the DMFC consisted of a methanol reservoir with a volume of 9 ml, a perfluorosulfonic acid-based ion-exchange membrane named “Nafion 117 membrane” serving as the pervaporation film, and a methanol vapor diffusion chamber made of the organic glass with the thickness of 10 mm and a CO_2 venting hole. A perforated polytetrafluoroethylene (PTFE) film with an open ratio of 24% was inserted between the Nafion 117 membrane and the vapor diffusion chamber to control the evaporation rate of methanol. Several layers of the hydrophobic micro-filtration membrane with the pore size of $0.45 \mu\text{m}$ and the thickness of $100 \mu\text{m}$ were used as the VTL, which were fixed in the vapor diffusion chamber to further adjust the methanol transport rate. The MEA was sandwiched between the anode and cathode flow field plates, which were made of 304 stainless steel plates coated with a thin gold layer. The open ratio, channel width and rib width of the flow field plate were, respectively, 50%, 1.0 mm and 0.9 mm. At the outside of the cathode flow field, several layers of the micro-filtration membrane were used as the WML to manage the mass transport of water.

2.2. MEA preparation

In the design, Toray 090 carbon paper with the thickness of $275 \mu\text{m}$ was used as the anode and cathode gas diffusion layers (GDL). The GDL was then treated with PTFE with a PTFE loading of 17 wt.%. After that, the carbon powder ink was sprayed onto the GDL surface to form a microporous layer (MPL) with a PTFE loading of 20 wt.%. The Pt–Ru alloy powder (molecule ratio 1:1) and the Pt/C (60 wt.% Pt) powder from Johnson Matthey® were used as the anode and cathode catalyst. The catalyst ink was prepared by the method reported elsewhere [30]. And the catalyst ink was then sprayed to the MPL surface to form the catalyst layer. The loading of the anode catalyst was about 4.0 mg cm^{-2} and the Nafion ionomer content in the catalyst was about 15 wt.%. The loading of cathode Pt catalyst was about 2.5 mg cm^{-2} and the Nafion ionomer content was also controlled at 15 wt.%. Nafion 117 membrane with a thickness of $180 \mu\text{m}$ was pretreated by the method reported in Ref. [31]. Finally, the MEA, with an active area of $2.0 \text{ cm} \times 2.0 \text{ cm}$, was fabricated by hot-pressing the pretreated Nafion 117 membrane

together with the anode and cathode gas diffusion electrodes at 135 °C and 4.0 MPa for 4 min.

2.3. Electrochemical instrumentation and test conditions

AutoLab PGSTAT302 (Eco Chemie, The Netherlands) Electrochemical work station interfaced to a computer was used to record the experimental results of the DMFC and control the operation conditions. In order to activate the fuel cell, the MEA was installed in an active DMFC fixture with 1.0 M methanol solution supplied to the anode channel and pure oxygen fed to the cathode side. The cell was discharged at the current density of 10 mA cm⁻² for 24 h at 30 °C. The constant voltage discharging method was employed to obtain the current–voltage (*I*–*V*) curves. For each point on the *I*–*V* curve, a 400 s waiting time was adopted to guarantee the cell current reach stable. The *I*–*V* curve test was performed at room temperature of 25.0 °C and the ambient relative humidity of about 50%. Five thermocouples were, respectively, placed in the anode fuel reservoir, methanol vapor diffusion chamber, anode electrode, cathode electrode, and ambient to monitor the temperature change of each part.

3. Results and discussion

3.1. Effect of the anode VTL thickness

As mentioned earlier, the anode VTL was used to control the transport rate of methanol from the fuel reservoir to the anode CL. In this section, the effect of the anode VTL thickness on methanol transport as well as the overall cell performance were examined by changing its value from 0.7 mm to 1.9 mm, while keeping other parameters unchanged. The average temperature of the anode and cathode electrodes was controlled at 30 °C in order to isolate the effect of temperature change on the cell performance.

Fig. 2 shows the effect of the VTL thickness on the performance of the DMFC fed with 8 M, 16 M methanol solution and neat methanol. As shown in Fig. 2(a), for 8 M methanol solution, the severe concentration polarization appears on the *I*–*V* curve for each VTL thickness tested, indicating that the methanol supply to the anode CL is insufficient. With the increase in the VTL thickness, the limiting current density decreases because of the increased mass transport resistance of methanol. For example, with increasing the VTL thickness from 0.7 mm to 1.9 mm, the limiting current density decreases from about 42 mA cm⁻² to 36 mA cm⁻². The dependence of cell performance on the VTL thickness for 16 M methanol solution operation is presented in Fig. 2(b). It is seen that, compared with Fig. 2(a), the limiting current density significantly increases as the higher concentration of the methanol solution leads to the higher methanol evaporation rate through the pervaporation film. Consequently, the methanol transport rate from the reservoir to the anode CL is enhanced. However, the concentration polarization is also observed on the *I*–*V* curve, indicating that the 16 M methanol solution also cannot supply the sufficient methanol to the anode CL. Fig. 2(c) presents the cell performances for neat methanol operation. Clearly, in the figure, no concentration polarization region appears on the *I*–*V* curve when the VTL thickness is smaller than 1.1 mm. At a certain cell voltage, the current density of the DMFC with thinner VTL is smaller, which suggests that enhanced methanol crossover through the membrane is occurring under neat methanol operation. Also, it is seen from Fig. 2(c) that the DMFC with the VTL thickness of 1.5 mm shows the best performance.

The peak power density for each test is shown in Fig. 3. Clearly, the peak power density monotonically decreases with the increase in the VTL thickness when the methanol solution

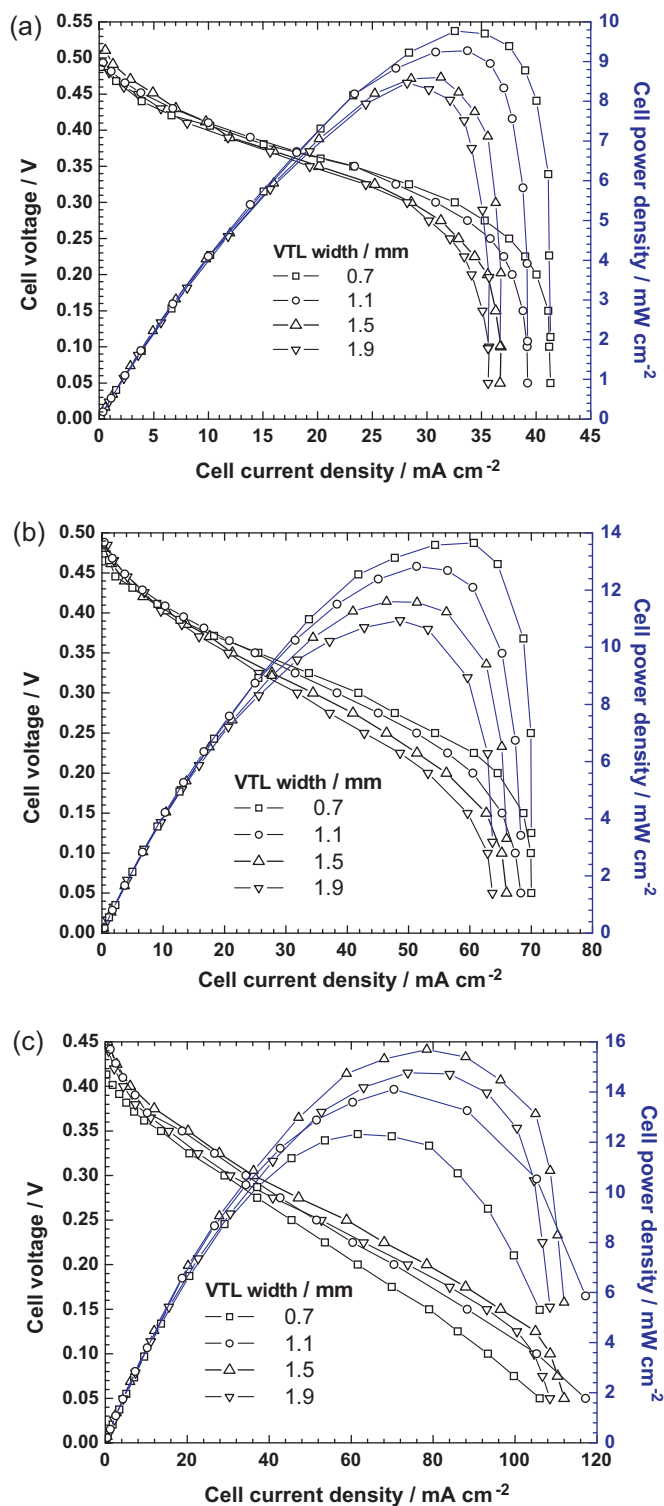


Fig. 2. Effects of the VTL thickness on the cell performance of the passive DMFC fed with methanol concentration of (a) 8 M, (b) 16 M, and (c) the neat methanol.

concentration in the reservoir is below 16 M. For instance, with the VTL thickness increasing from 0.7 mm to 1.9 mm, the peak power density decreases from 9.8 mW cm⁻² to 8.5 mW cm⁻² for 8 M methanol solution operation and decreases from 13.6 mW cm⁻² to 10.9 mW cm⁻² for the 16 M methanol solution operation. However, the variation of the peak power density with VTL thickness for the neat methanol operation exhibits different trends. As can be seen from the figure, the peak power density first increases with the

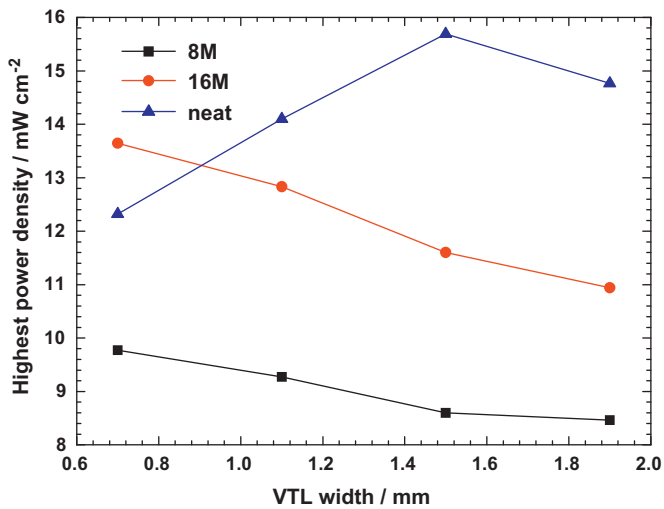


Fig. 3. Effects of the VTL thickness on the peak cell power densities of the passive DMFC fed with different methanol concentrations.

increase in the VTL thickness as the thicker VTL can suppress the methanol crossover rate, which benefits the improvement of the cell performance. When the VTL thickness reaches 1.5 mm, the peak power density reaches a maximum value of 15.7 mW cm^{-2} . With further thickening the VTL, the peak power density decreases. The above results indicate that for the cell structure designed in this work, the anode VTL thickness should be optimized to maximize the cell performance of the DMFC.

3.2. Effect of the cathode WML thickness

As the water in the anode CL is insufficient in a passive DMFC operated with highly concentrated methanol solution, it is necessary to recover part of the water generated in the cathode CL back to the anode. Herein, the cathode WML was employed to reduce the cathode water loss to the ambient air such that sufficient water could be reserved and recovered to the anode. In this section, the effect of cathode WML on overall cell performance was examined by varying its thickness from 0.0 to 2.3 mm with other parameters unchanged. The average temperature of the anode and cathode electrodes was also kept at 30°C . During the test, the variation of the relative ambient humidity is smaller than 5%. The water loss rate and cell performance are insensitive to this small change of the relative humidity. So the effect of the relative ambient humidity is neglected in the analysis and conclusions in the following sections.

Fig. 4 shows the effect of the cathode WML thickness on the cell performance of the passive DMFC fed with 8 M, 16 M methanol solution and neat methanol. Clearly, the cell performance is worst for the cells without the cathode WML. The reason can be explained as follows. On one hand, a large amount of water loss from the cathode CL leads to the decrease in the water content of the membrane, thus resulting in the increase in the cell resistance and consequently increasing the ohmic loss. In this experiment, we test the total resistance of the cell through the electrochemical impedance spectroscopy (EIS) method in the FRA function of the AutoLab electrochemical station. For example, under the neat methanol condition, the total cell resistance with no WML used at the cathode side of the cell is about $641 \text{ m}\Omega \text{ cm}^{-2}$. With the increase in the WML thickness, the total cell resistance becomes smaller. The total cell resistance with WML thickness of 1.1 mm and 1.9 mm are $550 \text{ m}\Omega \text{ cm}^{-2}$ and $510 \text{ m}\Omega \text{ cm}^{-2}$ respectively. On the other hand, too much water loss in the cathode CL causes the shortage of water in the anode CL, consequently retarding the reaction rate of anode MOR and exacerbating the problem of methanol crossover.

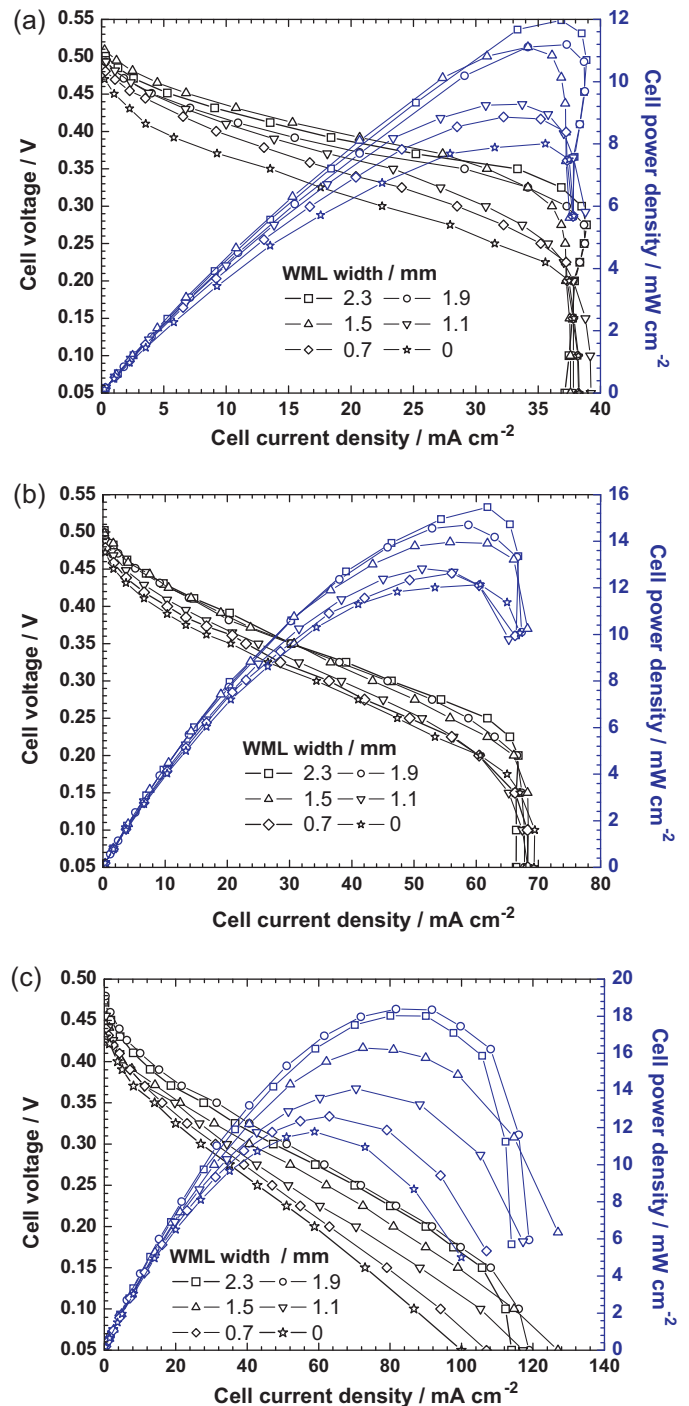


Fig. 4. Effects of the WML thickness on the cell performance of the passive DMFC fed with the methanol concentration of (a) 8 M, (b) 16 M, and (c) the neat methanol.

As shown in Fig. 4(a) and (b), the cell performance is improved by increasing the WML thickness as water loss at the cathode side can be effectively suppressed. Also, it is seen that the limiting current densities are insensitive to the WML thickness due to the fixed mass transport resistance of methanol through the DMFC anode. However, both the electrical resistance of the membrane and the methanol crossover greatly influence the cell performance, especially in the ohmic polarization region. With the increase in the WML thickness, the cell current density at a given cell voltage is increased because the ohmic loss in the membrane and the overpotential in the cathode CL resulting from the methanol crossover

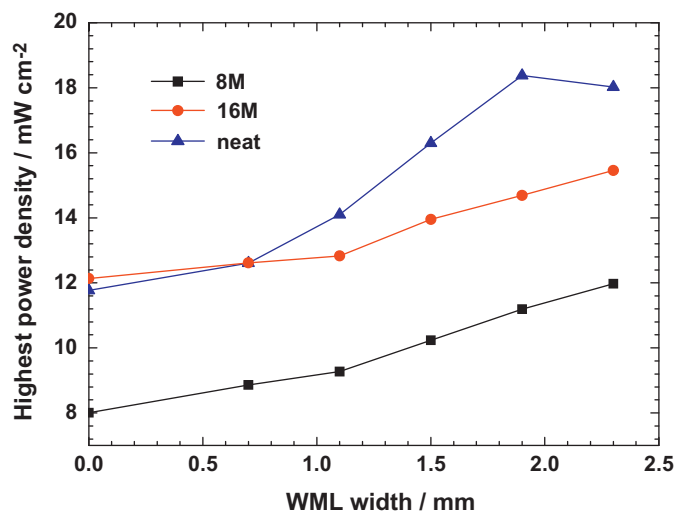


Fig. 5. Effects of the WML thickness on the peak cell power densities of the passive DMFC fed with different methanol concentrations.

are both reduced. Fig. 4(c) shows the cell performance of the passive DMFC fed with the neat methanol. Clearly, the maximum cell current density of the DMFC fed with neat methanol is much larger than that fed with 8 M and 16 M methanol solution because sufficient methanol can be supplied to the anode CL for the DMFC fed with neat methanol. Also, it can be seen from Fig. 4(c) that the cell performance is significantly improved with increasing the thickness of the WML from 0 to 1.9 mm. The DMFC with a 1.9 mm WML at the cathode side gives the optimum cell performance. Additionally, it is noticed that the limiting current densities of the passive DMFC with the WML thickness of 1.9 mm and 2.3 mm are smaller than the cell current density of the passive DMFC with WML thickness of 1.5 mm at the cell voltage of 0.05 V. This can be explained by the following reason. When the WML is too thick, the mass transport resistance of oxygen through the WML is high, which lowers the oxygen concentration in the cathode CL and increases the concentration polarization of the cathode oxygen reduction reaction (ORR) [27]. Also, the thick WML limits the transport of water vapor from the cathode CL to the ambient [11,25]. As a result, the water vapor produced in the cathode CL may condense into liquid water, causing the flooding problem and consequently deteriorating the cathode performance.

The peak power densities of the passive DMFC with different WML thicknesses are shown in Fig. 5. It can be seen from the figure that the peak power density monotonically increases with the increase in WML thickness for 8 M and 16 M methanol solution operation. For example, as the WML is increased from 0.0 mm to 2.3 mm, the peak power density of the passive DMFC fed with 8 M methanol solution increases from 8 mW cm⁻² to 12 mW cm⁻², while it is increased from 12.1 mW cm⁻² to 15.5 mW cm⁻² for the 16 M methanol solution operation. For neat methanol operation, however, the WML at the cathode has an optimum thickness of 1.9 mm, and the corresponding peak power density is 18.4 mW cm⁻². Further increase in the WML thickness leads to a little decrease in the peak power density because of the increased transport resistance of oxygen and water at the cathode side.

3.3. Temperature variation and heat transfer

In this section, we focus on investigating the heat transfer behavior in the passive high-concentration DMFC. The variations of the cell temperature under different operating conditions were recorded and analyzed. In the test, the thickness of the anode VTL was fixed at 1.1 mm and the cathode WML thickness is 1.5 mm.

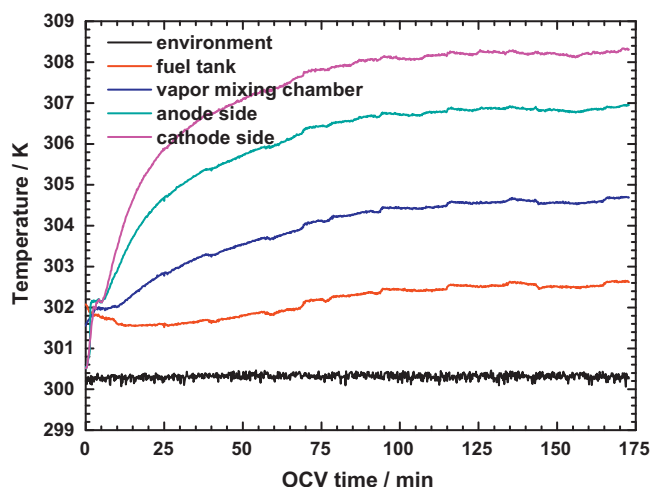


Fig. 6. Temperature variation in the different components of the passive vapor-fed high-concentration DMFC fed with neat methanol at the open circuit condition.

3.3.1. Open circuit condition

The time-dependent temperature variations at different locations in the passive DMFC fed with neat methanol are shown in Fig. 6. It can be seen that the temperature at each location starts to rise as soon as the neat methanol is fed to the reservoir. It reaches the stable value about 2 h later, indicating the balance between the heat generation and the heat loss from the passive DMFC to the ambient. Also, it is seen from the figure that the temperature in the cathode electrode is the highest. This is due to the reason that when the fuel cell is under the open circuit condition, no electrochemical reactions occur in the anode CL and thus all the heat is generated in the cathode CL due to the problem of methanol crossover. Generally, the stable temperature in the cathode electrode is about 8 K higher than the ambient temperature. The temperature is gradually lowered from the cathode electrode to the anode fuel reservoir due to the increased heat transfer resistance. The temperature distribution in different components of the passive DMFC reflects the behaviors of heat generation and transport in the fuel cell.

The comparison of the cell temperature at the cathode electrode of the passive DMFC fed with 8 M, 16 M methanol solution and neat methanol is also presented in Fig. 7. It can be seen from the figure that the variation trends of temperature through the DMFC with different methanol feed concentrations are similar. It takes about 2 h

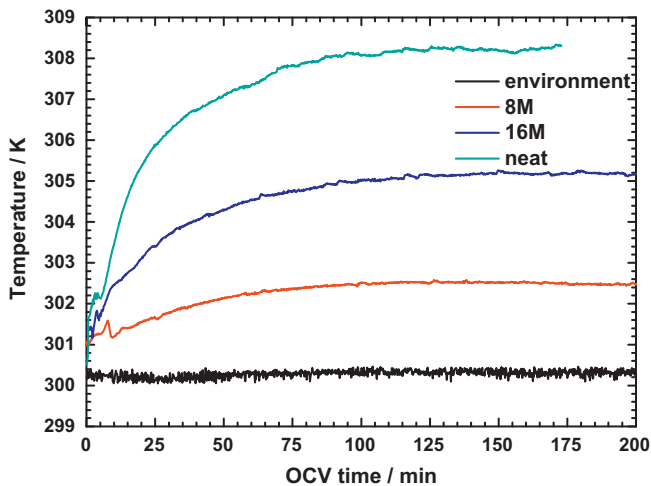


Fig. 7. Temperature variation of the passive vapor-fed high-concentration DMFC fed with different methanol solution concentrations at the open circuit condition.

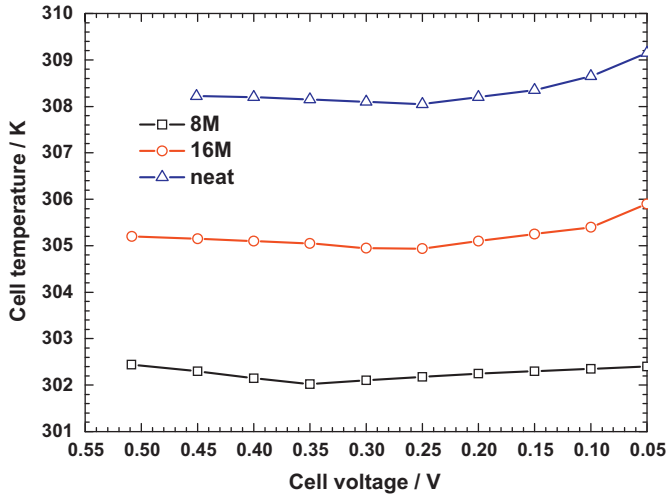


Fig. 8. Temperature profiles of the passive vapor-feed high-concentration DMFC at various discharging voltages.

for the cell temperature to reach equilibrium. With the increase in the methanol feeding concentration, the cell temperature increases because of the increased methanol crossover to the cathode. This is in agreement with the analysis in our former work [32]. The temperature differences between the cathode electrode and the ambient for the 8 M, 16 M methanol solution and neat methanol are 2.3 K, 5 K, and 8 K, respectively. Although methanol crossover causes the loss of fuel, it should be noted that the rise of temperature resulting from the methanol oxidation reaction in the cathode CL can promote the electrochemical reaction in the CLs, which may in turn improve the cell performance.

3.3.2. Constant voltage discharging condition

The stable cell temperatures of the passive DMFC under constant voltage discharging condition were also measured to analyze the heat transport behavior in the DMFC. In the tests, the DMFC was controlled to discharge under different voltages for 2 h in order to achieve the stable cell temperature. Fig. 8 shows the profiles of the stable temperature of the passive DMFC at different discharging voltages. It can be seen that the temperature variation with the cell voltage is quite different with that in the traditional passive DMFC [3]. In the later, a significant temperature increase can be observed when the DMFC is discharged at a low cell voltage. This is because the main transport resistance of methanol in the traditional passive DMFC exists in the anode GDL and membrane. At the lower cell voltage, methanol crossover rate becomes smaller. More methanol is consumed in the anode CL. Thus, the gradient of methanol concentration in the anode GDL becomes larger. The methanol transport flux increases significantly, which results in a higher heat generation rate and consequently a higher cell temperature. However, in the passive vapor-feed high-concentration DMFC, the temperature variations under different operating voltages are quite small as indicated in Fig. 8. Also, it is noticed that the cell temperature first drops with the decrease in the discharging voltage and then rises with further decreasing the discharging voltage. For instance, for the 8 M methanol feeding concentration, the cell temperature reaches the lowest value at 0.35 V, which is about 0.4 K lower than the cell temperature under open circuit condition. However, the cell temperature rises to about 302.4 K at cell voltage of 0.05 V. Similar trends can be observed for the 16 M and neat methanol operation. The lowest cell temperatures for these two cases appear at the cell voltage of 0.25 V. The variation trend of cell temperature shown in Fig. 8 can be explained by analyzing methanol transport behaviors in a passive vapor-feed high-concentration DMFC. The methanol

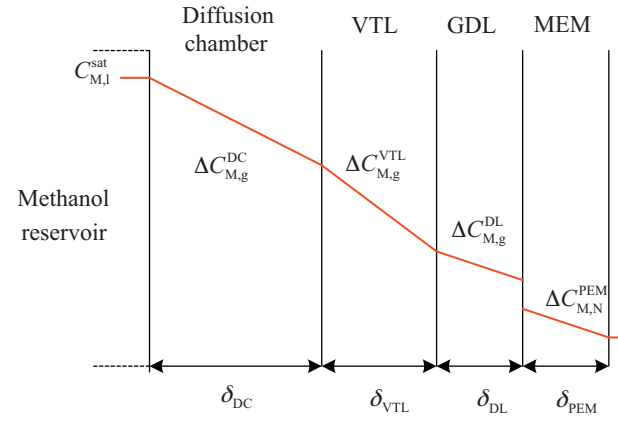


Fig. 9. Schematic of the methanol transport in the passive vapor-feed high-concentration DMFC.

transport through the cell structure illustrated in Fig. 1 is shown in Fig. 9 and the structure parameters and physical properties are listed in Table 1. The evaporation rate of liquid methanol through the pervaporation film can be expressed by

$$J_M^V = A\xi h(C_{M,I}^{sat} - C_{M,g}) \tag{1}$$

where J is the methanol evaporation rate, A is the area of the pervaporation film, ξ is the open ratio of the PTFE film, h is the mass transport coefficient and C is the methanol vapor concentration. The diffusion flux of methanol vapor through each components of this passive vapor-feed DMFC can be written as follows:

$$\text{Diffusion chamber: } J_M^{DC} = A_{DC} D_{M,g} \frac{\Delta C_{M,g}^{DC}}{\delta_{DC}} \tag{2}$$

$$\text{VTL: } J_M^{VTL} = A_{VTL} D_{M,g} (\varepsilon_{VTL})^\beta \frac{\Delta C_{M,g}^{VTL}}{\delta_{VTL}} \tag{3}$$

$$\text{GDL: } J_M^{DL} = A_{DL} D_{M,g} (\varepsilon_{DL})^\beta \frac{\Delta C_{M,g}^{DL}}{\delta_{DL}} \tag{4}$$

$$\text{MEM: } J_M^{PEM} = A_{PEM} D_{M,N} \frac{\Delta C_{M,N}^{PEM}}{\delta_{PEM}} \tag{5}$$

where D denotes the diffusion coefficient of methanol vapor, ε is the porosity of each component, and δ is the thickness of each component.

Under open circuit condition, the fluxes of methanol transported through different components are equal, which gives

$$J_M^V = J_M^{DC} = J_M^{VTL} = J_M^{DL} = J_M^{PEM} \tag{6}$$

When the cell is discharged at a certain cell voltage, we have

$$J_M^V = J_M^{DC} = J_M^{VTL} = J_M^{DL} \tag{7}$$

According to Eqs. (1)–(7) and the parameters listed in Table 1, it can be seen that the methanol transport resistance is mainly caused by the anode components including the pervaporation film [11],

Table 1 Structure parameters and the component physical properties of the vapor feed high concentration DMFC.

Components	Thickness	Porosity
Methanol vapor transport chamber	10 mm	1
VTL	0.7–1.9 mm	0.4
Rib	1 mm	1
GDL	0.25 mm	0.7
CL	0.02 mm	0.3
PEM	0.18 mm	0.3
WML	0.0–2.3 mm	0.4

the vapor diffusion chamber and the VTL. The transport resistance of methanol through MEA only contributes a quite small part of the total resistance. As a result, the change of the cell operation condition from open circuit operation to constant voltage discharging exhibits little impact on the total mass transport resistance of methanol. Consequently, the variation in the methanol transport flux is negligible. This behavior is reflected by the quite small temperature difference between the cells operated under different cell voltages. Also, it is found that the cell voltages, at which the cell temperature reaches the lowest values, are exactly the ones where the passive DMFC gives the peak power density. This can be explained by the following reason, part of the energy stored in the fuel is converted into useful work through external circuit when the passive DMFC is discharged at a certain voltage, and the rest is lost in the form of heat. The trade off between the useful work and the waste heat at different cell voltage determines the exact trend of the temperature profiles.

4. Conclusions

This paper reported the experimental study on the performance of a passive vapor-fed DMFC operated with highly concentrated fuel. The effects of anode VTL thickness and cathode WML thickness on the overall cell performance and the characteristics of heat and mass transport inside the cell were examined. The cell temperature variations at different working conditions were also recorded to analyze the heat generation and transfer processes in the cell. The salient findings are as follows:

- (1) The anode VTL can be used to carefully adjust the methanol transport rate to the anode CL. The passive DMFC can give an optimum cell performance at a proper thickness of the VTL when the DMFC is operated with neat methanol.
- (2) The cathode WML can help recover part of the water generated in the cathode CL back to the anode CL, thus benefiting the improvement of the cell performance. However, the cathode WML should not be too thick in order to avoid the severe concentration polarization due to the high oxygen transport resistance. Also, too thick WML may cause the condensation of the water vapor and raise the risk of water flooding problem.
- (3) The stable cell temperature under open circuit condition increases with the increase in the methanol concentration because of the higher methanol crossover rate. When the DMFC

is discharged, the variations of the stable cell temperature at different discharging voltages are quite small. This reflects that the methanol transport resistance in the MEA only contributes a small part of the total resistance in the passive DMFC components.

Acknowledgement

This work is supported by the National Natural Science Foundation of China (Nos. 51176155, 51106128).

References

- [1] G.J.K. Acres, J. Power Sources 100 (2001) 60–66.
- [2] C.K. Dyer, J. Power Sources 106 (2002) 31–34.
- [3] R. Chen, T.S. Zhao, J. Power Sources 167 (2007) 455–460.
- [4] Z. Miao, Y.L. He, X.L. Li, J.Q. Zou, J. Power Sources 185 (2008) 1233–1246.
- [5] Z. Miao, Y.L. He, J.Q. Zou, J. Power Sources 195 (2010) 3693–3708.
- [6] Z.H. Wang, C.Y. Wang, J. Electrochem. Soc. 150 (2003) A508–A519.
- [7] C. Xu, Transport Phenomena of Methanol and Water in Liquid Feed Direct Methanol Fuel Cells, Hong Kong University of Science and Technology, Hong Kong, 2009.
- [8] W.W. Yang, T.S. Zhao, Electrochim. Acta 52 (2007) 6125–6140.
- [9] Y.L. He, X.L. Li, Z. Miao, Y.W. Liu, Appl. Therm. Eng. 29 (2009) 1998.
- [10] T.S. Zhao, W.W. Yang, R. Chen, Q.X. Wu, J. Power Sources 195 (2010) 3451–3462.
- [11] W.W. Yang, T.S. Zhao, Q.W. Wu, Int. J. Hydrogen Energy 36 (2011) 6899–6913.
- [12] M.A. Abdelkareem, N. Morohashi, N. Nakagawa, J. Power Sources 172 (2007) 659–665.
- [13] M.A. Abdelkareem, N. Nakagawa, J. Power Sources 162 (2006) 114–123.
- [14] N. Nakagawa, M.A. Abdelkareem, K. Sekimoto, J. Power Sources 160 (2006) 105–115.
- [15] X. Ren, J.J. Becerra, R.S. Hirsch, S. Gottesfeld, U.S. Pat. (2004) 2004/0209136A1.
- [16] H.K. Kim, J. Power Sources 162 (2006) 1232–1235.
- [17] S. Eccarius, F. Krause, K. Beard, C. Agert, J. Power Sources 182 (2008) 565–579.
- [18] S. Eccarius, X. Tian, F. Krause, C. Agert, J. Micromech. Microeng. 18 (2008) 104010.
- [19] Q.X. Wu, T.S. Zhao, R. Chen, W.W. Yang, J. Micromech. Microeng. 20 (2010) 045014.
- [20] C.E. Shaffer, C.Y. Wang, J. Power Sources 195 (2010) 4185–4195.
- [21] H. Bahrami, A. Faghri, J. Fuel Cell Sci. Technol. 8 (2011) 021011.
- [22] C. Xu, A. Faghri, J. Power Sources 195 (2010) 7011–7024.
- [23] C. Xu, A. Faghri, X. Li, Int. J. Hydrogen Energy 36 (2011) 8468–8477.
- [24] C. Xu, A. Faghri, X. Li, J. Electrochem. Soc. 157 (2010) B1109–B1117.
- [25] Q.X. Wu, T.S. Zhao, Int. J. Hydrogen Energy 36 (2011) 5644–5654.
- [26] Q.X. Wu, T.S. Zhao, R. Chen, W.W. Yang, Int. J. Hydrogen Energy 35 (2010) 10547–10555.
- [27] Q.X. Wu, T.S. Zhao, W.W. Yang, Int. J. Heat Mass Transfer 54 (2011) 1132–1143.
- [28] X. Li, A. Faghri, C. Xu, J. Power Sources 195 (2010) 8202–8208.
- [29] X. Li, A. Faghri, C. Xu, Int. J. Hydrogen Energy 35 (2010) 8690–8698.
- [30] C. Xu, T.S. Zhao, Y.L. He, J. Power Sources 171 (2007) 268–274.
- [31] H. Yang, T.S. Zhao, Q. Ye, J. Power Sources 139 (2005) 79–90.
- [32] Z. Miao, Y.L. He, T.S. Zhao, W.Q. Tao, Front. Heat Mass Transfer 2 (2011) 013001.